

COMBINED PHOTOTHERMAL AND NANO-CHEMOTHERAPY IN TREATMENT OF INDUCED ORAL SQUAMOUS CELL CARCINOMA IN HAMSTERS

Randa Hamed El-Sherbiny¹, Magda Mohamed Aly Hassan², Wafaa Hassanein El-Hossary³, Mona Saad Shata⁴.

DOI: 10.21608/dsu.2021.32548.1040

Manuscript ID: DSU-2006-1040 (R1)

KEYWORDS

Folate, Gold nanoparticles,
Oral squamous cell carcinoma,
Thymoquinone.

• E-mail address:
hms.randa@yahoo.com

1. Assistant Lecturer of Oral Pathology, PhD student, Department of Oral Pathology, Faculty of Dentistry, Suez Canal University, Ismailia, Egypt.
2. Professor of Oral Pathology, Department of Oral Pathology, Faculty of Dentistry, Suez Canal University, Ismailia, Egypt.
3. Associate Professor of Oral Pathology, Department of Oral Pathology, Faculty of Dentistry, Suez Canal University, Ismailia, Egypt.
4. Lecturer of Oral Pathology, Department of Oral Pathology, Faculty of Dentistry, Suez Canal University, Ismailia, Egypt.

ABSTRACT

Introduction: Oral squamous cell carcinoma (OSCC) shows unsatisfied survival rate which remains not changed over the last years. Thymoquinone (TQ) is a phytochemical, and many studies proved its promising therapeutic effect against OSCC. Gold nanorod (GNR) is a photothermal agent, has an efficient near-infrared heat conversion and induces ablation of solid tumors. The combination of photothermal therapy (PTT) and chemotherapy can enhance synergistic effects that markedly exceed the sum of individual treatments alone. **Aim:** this study aimed to evaluate the effect of combined photothermal and nano chemotherapy in treatment of induced oral squamous cell carcinoma in hamsters. **Material and Methods:** In the present study, the combined drug GNR/NTQ loaded on (poly) (lactic-co-glycolic acid) (PLGA) was prepared. The targeting agent, folate or folic acid (FA), was conjugated to the prepared nanoparticles. The therapeutic activity of the drug against chemically-induced OSCC in hamster buccal pouches was evaluated by clinical observations, tumor volume analysis, histopathological alterations and blood analysis. **Results:** The combined drug (GNR/NTQ/PLGA/FA/laser) had the highest therapeutic activity compared to individual treatments. It significantly ablated and regressed tumor size in chemically-induced OSCC in the hamster model as compared to the other preparations; GNR/NTQ/PLGA/FA without laser, GNR/ PLGA/FA/laser and NTQ/PLGA/FA/laser. **Conclusion:** Compared to the single PTT or nanochemotherapy, the combined PTT/nanochemotherapy with laser provides better therapeutic effects against OSCC

INTRODUCTION

Worldwide, oral cancer is the eleventh cancer in rate among population.⁽¹⁾ Oral squamous cell carcinoma (OSCC) represents more than 90% of all oral cancers.⁽²⁾ Oral carcinogenesis is due to exposure to multiple risk factors, which lead to genetic mutations⁽³⁾.

In early stages, more than 80% of patients can be survived by treatment but it will be incurable with advanced stages; the overall survival rate is less than 50%.⁽⁴⁾ Traditional treatments may cause severe facial defects and need to be replaced by gentle treatments.⁽⁵⁾ Photothermal therapy (PTT) is one of the recent techniques that used nanoparticles and can improve that unsatisfied outcome⁽⁶⁾.

The most known model to study alteration in histopathology and biochemistry in oral cancer is hamster buccal pouch with induction of cancer by DMBA carcinogen⁽⁷⁾. The resulting malignant tumors in the hamster mimic human oral tumors, morphologically, histopathologically as well as at the molecular level⁽⁸⁾.

Thymoquinone (TQ) is extracted from *Nigella sativa* plant and it showed strong anticancer effects⁽⁹⁾. It has multi-targeting effects, TQ meddles with a wide range of tumorigenic effect and interfere with carcinogenesis, malignant growth, angiogenesis invasion and migration⁽¹⁰⁾. TQ has poor bioavailability due to its rapid elimination and slow absorption, so it has also low bioavailability⁽¹¹⁾. Nanoparticles forms of TQ can improve its bioavailability. It is called nano-chemoprevention or nano-chemotherapy⁽¹²⁾. TQ nanoparticles (NTQ) have a promising effect than TQ alone, because of better focusing on cancer hallmarks, and improve bioavailability⁽¹³⁾.

Plasmonic photothermal therapy (PPTT) is a type of PTT induced by GNPs. As excitation of electrons followed by rapid relaxation can produce strong heat effect that can destroy targeted cancer cells⁽¹⁴⁾. Of all GNPs, gold nanorods (GNRs) are the best in applications *in vivo* and *in vitro* since light penetration is in the average of 600–1200 nm⁽¹⁵⁾. GNRs in the second near-infrared (NIR) window, are allowing them to penetrate up to 10 cm in tissues⁽¹⁶⁾. This size of GNRs is about 10 nm in width and 40 nm in length which is proper with tumors leaky vasculature⁽¹⁷⁾. GNRs have low absorption degree in hemoglobin, lipids and water⁽¹⁸⁾. They allow tumor treatment with little damage to the surrounding normal tissues^(19,20).

Strategies for combined PTT and chemotherapy have a great ability to cause an increase in treatment efficacy with minimization of off-target effects⁽²¹⁾.

Hyperthermia leads to increases permeability of cell membrane and vascular system⁽²²⁾. These changes can increase the effect of chemotherapeutic drugs⁽²³⁾.

Folic acid (pteroylglutamic acid; C₁₉H₁₉N₇O₆) is a promising active target, where cells of cancer have tendency to overexpress the folate-receptor as they vastly require folate⁽²⁴⁾. Its expression is limited in organs and tissues that are healthy⁽²⁵⁾. Folate receptors have high expression in cervical, ovarian, epithelial, and colorectal tumors⁽²⁶⁾. Folic acid has high stability over a wide scale of temperatures and pH values⁽²⁷⁾. Poly (lactic-co-glycolic acid) (PLGA) is one of the best used nanoparticulate carriers. It is a biodegradable copolymer, which decompose to H₂O and CO₂⁽²⁸⁾.

The development of an effective system of GNRs and NTQ loaded on PLGA with the active targeting agent FA, introduced to facilitate combined therapy of PTT and nanochemotherapy. This combination was applied on chemically-induced OSCC in hamsters' buccal pouches, to offer better therapeutic efficacy compared with either photothermal therapy or chemotherapy.

MATERIAL AND METHODS

Agreement of Research Ethics Committee at Faculty of Dentistry/Suez Canal University was gained before starting the experiment (49/2017).

Chemicals: The carcinogen 0.5% 7,12-dimethylbenz (a) anthracene (DMBA) dissolved in heavy mineral oil (U.S.P), Chlorauric acid, Poly [ethylene glycol], Thymoquinone, Folic acid and Phosphate-buffered saline (PBS), PH=7.4. All the previous chemicals were from Sigma-Aldrich Company, Saint Louiss, USA.

Drugs' preparation:

Preparation of TQ-loaded nanocapsules (NTQ): ⁽²⁹⁾ The capsules of NTQ were prepared using water and oil emulsion plus evaporation solvent method. TQ (1.3 mg/ml dissolved in 135 μ L of anhydrous chloroform) was mixed with PLGA/PEG/FA (25 mg/ml) dissolved in 135 μ L chloroform.

Preparation of GNRs-loaded nanocapsules: ⁽³⁰⁾ The seed-mediated growth method was used for preparation of GNRs. Then a mix of PLGA/PEG/FA solution that dissolved in chloroform was added to colloid of GNRs. The nanocapsules (GNR/PLGA/PEG/FA) were collected by centrifugation with high-speed then washed with PBS.

Preparation of NTQ/GNRs-loaded nanocapsules: Thymoquinone was mixed in PLGA/PEG/FA and then added slowly to GNRs colloid. The nanocapsules (TQ/GNR/PLGA//FA) were collected using high-speed centrifugation.

The morphological characterization of the prepared combined drug (GNR/NTQ/PLGA/FA) was done by images from transmission electron microscopy (TEM)

Experimental design: The experiment was done at the Animal House of Faculty of Dentistry, Suez Canal University, Ismailia, Egypt. Sixty male Syrian golden hamsters (*Mesocricetus auratus*), weighing 90-110 grams and aged 6-8 weeks, and were housed, five per cage. All hamsters were given pellets made up of seeds, grains and cracked corn, and tap water *ad libitum*. They were kept in a controlled environment under standard conditions of temperature and humidity with an alternating light/dark cycles with 12 hours- intervals. Animals were divided into control groups and treated groups as follow:

Control groups: Group A1 (n=10): served as the negative control group. Five animals were euthanized at day zero and five were euthanized at end of the experiment. **Group A2:** (n=10): served as positive control group. Animals were painted three times per week, in the left buccal pouch, with the carcinogen (DMBA) for 12 weeks then followed up for another 4 weeks. A camel hairbrush, number 4, was used for painting ⁽³¹⁾.

Treated groups: Group B (n=40) all hamsters were painted weekly (three times/week), in the left buccal pouch with DMBA for 12 weeks. Then were injected intraperitoneally (i.p) as following: **Group B1:** (n=10) hamsters were injected by GNR/NTQ/PLGA/FA (1.5mg/kg body weight of GNR, and TQ which was 0.2 mg/kg. laser exposure was done after 24 hours (2.5 W/cm² for 10 min). **Group B2:** (n=10) animals were injected by GNR/NTQ/PLGA/FA (no laser exposure). **Group B3:** (n=10) animals were injected by GNR/PLGA/FA (1.5mg/kg body weight). After 24 hours, the painted pouches were exposed to laser as in group B1. **Group B4:** (n=10) animals were injected by NTQ/PLGA/FA (0.2 mg/kg body weight).

In all treated groups, the dose/week given to each hamster was 0.2mL/100g body weight. Two doses were given in each treated group where one dose was given at the 13th week and the second dose in the 14th week. Follow up were done till the end of 16th week (end of the experiment). To measure tumor size and laser application, animals were anesthetized by ketamine 50mg/kg mixed with xylazine, (xylazine) 5mg/kg, to prevent pain and control animals' movement. Hamsters were euthanized by inhalation of a lethal dose of diethyl ether (cotton-soaked) in a tightly closed container.

Clinical findings: Hamsters were examined every day for survival, activity behavior and motion impairments.

Assessment of tumor volume: caliper was used to measure tumor volume in horizontal and vertical directions. The formula used was $V = (W^2 * L) / 2$. V means tumor volume, L means tumor length and W means tumor width⁽³²⁾. Tumor volumes were measured at two different time points, at end of 12th and 16th weeks, for all experimental groups (A2 and B).

Hematological investigation: Before euthanization and under anaesthesia, a blood sample (2ml) was withdrawn from each animal for evaluating complete blood count (CBC), as well as liver and kidney toxicity.

Histopathological examination: After surgical excision of right and left pouches, then they were fixed in 10% neutral buffer formalin and embedded in paraffin wax. By microtome 5µm sections were obtained, and stained with hematoxylin and eosin. Examination was done by a light microscope.

Statistical analysis: To compare results of tumor volumes, Two-way ANOVA test followed by Duncan Multiple Range Tests were done. While for blood results, One-way ANOVA test followed by Duncan Multiple Range Tests were done.

RESULTS

Size and shape of the combined drug GNR/NTQ/PLGA/FA nanocapsules: The images of transmission electron microscopy (TEM) recorded that the nanocapsules (NCs) were highly monodispersed, well-defined and uniform in shape with regular distribution. Capsule's size ranged from 115-180 nm and the morphology was spherical in shape (pan cake shape of PLGA shell). Numerous GNRs and NTQ were successfully encapsulated in the PLGA NCs while FA appeared at the border of the NCs as shown in Figure 1.

Clinical findings: Animals painted with DMBA showed hair loss and marked weight loss,

red macules and papules, reduced length of the left pouches (about 2cm) compared to the control pouches (5 cm). Papillary overgrowths were found intra-orally and periorally which increased in size by end of the experiment. By end of week 16, animals treated with GNR/NTQ/laser and GNR/laser (groups B1 and B3), showed marked weight regain and decrease in papillary overgrowths' size up to complete ablation of small tumors in group B1. Animals treated with GNR/NTQ without laser and NTQ alone (groups B2 and B4) showed no improvement compared to group A2.

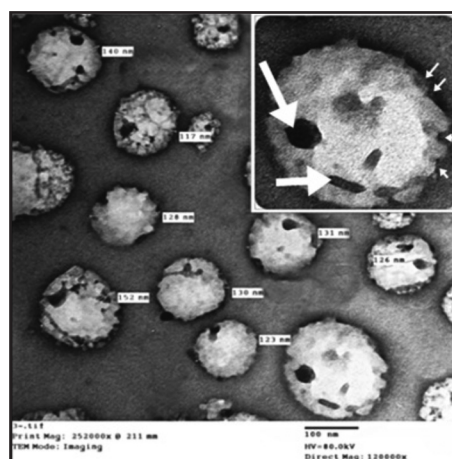


Fig. (1) TEM image of the prepared combined chemo/photothermal drug (GNR/TQ/PLGA/PEG/FA). The average diameter of the capsules ranges from 115-180 nm. Inset: Image of single capsule shows pancake shaped PLGA shell, the black structures are the GNRs and NTQ (large arrows). The black dots at the borders of NCs represent FA (small arrows). Magnification $\times 12000$

Assessment of tumor volume: *Difference between tumor volumes at 12th and 16th weeks in the same group* showed significant increase in the mean tumor volumes by end of the 16th week in groups A2 (DMBA), B2 (GNR/NTQ/no laser) and B4 (NTQ) (1.03 ± 0.17 , 0.75 ± 0.07 and 0.56 ± 0.09 , respectively) in comparison to their mean at 12th week (0.25 ± 0.06 , 0.26 ± 0.06 and 0.3 ± 0.06 , respectively). Significant

decrease was recorded in the mean tumor volumes of B1 (GNR/NTQ/laser) and B3 (GNR/laser) groups by end of the 16th week (0.00 ± 0.00 and 0.03 ± 0.01 , respectively) in comparison to their mean at 12th week (0.31 ± 0.09 and 0.35 ± 0.05 , respectively) as shown in Figure 2 ($p \leq 0.05$).

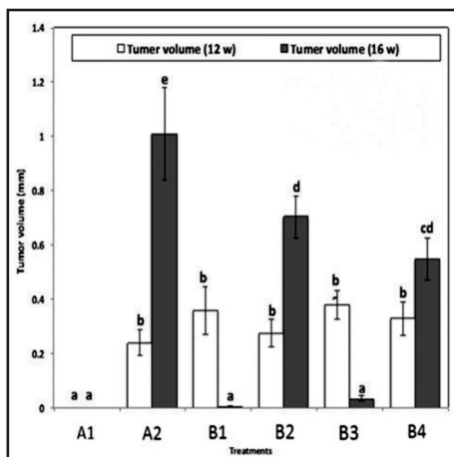


Fig. (2) Shows mean tumor volumes in hamsters' pouches at different treatments and time points before (12 weeks) and after treatments (16 weeks). (A1: Negative control group, A2: DMBA group, B1: GNR/NTQ/PLGA/FA/laser, B2: GNR/NTQ/ PLGA/FA/no laser, B3: GNR/PLGA/FA/laser and B4: NTQ PLGA/FA).

Tumor volumes differences at end of 16th week showed no significant difference between group A1 (negative control), B1 (GNR/NTQ/laser) and B3 (GNR/laser). However, highly significant difference between groups B1 and B3 compared to A2. On the other hand, statistically significant difference was recorded between groups B2 (GNR/NTQ/ no laser) and B4 (NTQ) compared to A2 as shown in Figure 2 ($p \leq 0.05$). Data of tumor volume were collected and organized using SPSS and Microsoft excel 2016. Inferential statistics for evaluating and comparing between different treatments at different time points were carried out using two-way analysis of variance (ANOVA). It was followed

by Duncan multiple range tests (DMRTs) to compare between groups in tumor volume results Data analyses were carried out using computer software statistical package for social science (SPSS) IBM-SPSS ver. 23.0 for Mac OS.

Histopathologic results (Figures 3):

Group A1 (negative control) showed normal mucosa composed of four distinct layers. Group A2 (DMBA group) showed well to moderate differentiated oral squamous cell carcinoma (OSCC) in the form of numerous large papillomatous overgrowths with multiple invading malignant epithelial islands into the connective tissue. The rest of the epithelium showed hyperplasia and hyperkeratinization with dysplasia.

Group B1 (GNR/NTQ with laser) showed small papillomatous lesions of mild to severe dysplasia. The rest of epithelial surface showed hyperplasia and hyperkeratinization with variable degrees of dysplasia (from mild to severe). Apoptotic cells were found; as smaller cells with nuclear fragmentation, marked cytoplasm condensation with delineated cell borders.

Group B2 (GNR/NTQ without laser) showed multiple papillomatous overgrowths with well to moderate differentiated OSCC. The rest of the epithelium showed hyperplasia and hyperkeratinization with moderate to severe dysplasia.

Group B3 (GNR/laser) showed small multiple papillomatous lesions that showed carcinoma in situ, as well as apoptotic cells.

Group B4 (NTQ) showed multiple papillomatous overgrowths with well to moderate differentiated OSCC. The rest of the pouches' lining showed focal areas of epithelial hyperplasia and hyperkeratinization with moderate to severe dysplasia.

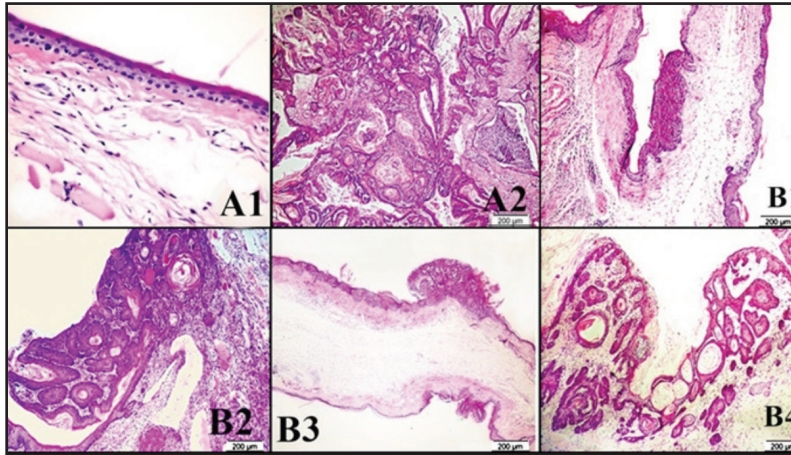


Fig. (3) A combined picture representing histopathologic sections, of all groups at end of the 16th week. A1: untreated group (H&E, x20), A2: DMBA group, B1: GNR/NTQ/PLGA/FA/laser group, B2: GNR/NTQ/PLGA/FA (no laser) group, B3: GNR/PLGA/FA/laser group, and B4: NTQ/PLGA/FA group (from A2-B4: H&E x4).

Results of blood analysis: Liver function tests (ALT and AST values) were increased significantly with GNR/NTQ/laser and GNR/laser. On the other hand, ALT and AST values decreased significantly in the positive control group, GNR/NTQ without laser and NTQ, as shown in (Table 1). **Kidney function tests** showed that creatinine level was significantly increased in positive control group and urea levels significantly decreased in positive control group. While no statistically significant difference in the mean values of uric acid between groups as shown in Table 1 ($p \leq 0.05$). In blood count results (table 2), **total white blood cells (WBCs) count** was increased significantly in the GNR/NTQ/laser and GNR/laser groups. While it was highly increased significantly in DMBA group, and very

highly increased significantly in GNR/NTQ without laser and NTQ groups ($p \leq 0.05$). **Platelets count (plt)** showed no significant difference in GNR/NTQ/laser group. While it was increased significantly in GNR/laser group, and very highly increased significantly in DMBA, GNR/NTQ without laser and NTQ groups ($p \leq 0.05$). **Hemoglobin (Hb) level** was decreased significantly in GNR/NTQ/laser group. It was very highly significantly decreased in DMBA, GNR/NTQ without laser, GNR/laser and NTQ groups compared to negative control group ($p \leq 0.05$). **Red blood corpuscles (RBCs)** were decreased significantly in GNR/NTQ/laser and GNR/laser groups and it was very highly significantly decreased in DMBA, GNR/NTQ without laser and NTQ groups ($p \leq 0.05$).

Table (1) Statistical analysis of liver and kidney function tests of all hamsters under different treatments at week 16:

Treatments	ALT (U/L)	AST (U/L)	Creatinine (mg/dl)	Urea (mg/dl)	Uric acid (mg/dl)
A1	27.40 ± 1.97 ^b	45.00 ± 1.58 ^b	0.21 ± 0.06 ^a	42.90 ± 0.67 ^b	6.09 ± 0.29 ^a
A2	0.70 ± 0.47 ^a	1.50 ± 0.78 ^a	0.34 ± 0.08 ^b	41.10 ± 0.82 ^a	6.77 ± 0.27 ^a
B1	49.80 ± 4.96 ^c	140.90 ± 27.0 ^d	0.12 ± 0.01 ^a	44.20 ± 0.29 ^b	5.87 ± 0.34 ^a
B2	6.20 ± 1.62 ^a	9.10 ± 1.95 ^a	0.15 ± 0.03 ^a	44.00 ± 0.54 ^b	6.06 ± 0.31 ^a
B3	47.80 ± 4.52 ^c	100.10 ± 2.09 ^c	0.10 ± 0.00 ^a	43.90 ± 0.46 ^b	5.84 ± 0.39 ^a
B4	7.30 ± 1.40 ^a	4.10 ± 1.43 ^a	0.10 ± 0.00 ^a	42.80 ± 0.92 ^b	5.78 ± 0.36 ^a

Different between treatments groups was assessed by one-way analysis of variance and followed by DMRTs. Means followed by different letters are significantly different according to DMRTs at $p \leq 0.05$.

Table (2) Statistical analysis of WBCs, plt count, Hb and RBCs of all groups at end of the experiment (16 weeks):

Treatments	WBCs ($10^3/\mu\text{l}$)	Plt ($10^3/\mu\text{l}$)	HB (g/dL)	RBCs ($10^6/\mu\text{l}$)
A1	5.19 ± 0.20^a	330.00 ± 16.72^a	12.93 ± 0.40^d	8.51 ± 0.27^d
A2	9.87 ± 0.43^c	1517.60 ± 137^d	6.26 ± 0.32^{ab}	3.12 ± 0.25^a
B1	8.74 ± 0.20^b	328.50 ± 36.91^a	10.24 ± 0.23^c	6.57 ± 0.12^c
B2	11.94 ± 0.16^d	1052.4 ± 67.92^c	5.93 ± 0.12^a	3.54 ± 0.27^a
B3	8.74 ± 0.20^b	741.00 ± 69.35^b	6.95 ± 0.09^b	4.77 ± 0.34^b
B4	11.14 ± 0.45^d	1108.8 ± 66.35^c	6.00 ± 0.20^a	3.45 ± 0.30^a

Different between treatments groups was assessed by one-way analysis of variance and followed by DMRTs. Means followed by different letters are significantly different according to DMRTs at $p \leq 0.05$.

Significant at $p < 0.05$. Data represented as mean \pm standard error for mean. Difference between treatment groups was assessed by two-way analysis of variance and followed by Duncan's multiple range tests (DMRTs). Means followed by different letters are significantly different according to DMRTs at $p \leq 0.05$.

DISCUSSION

Combination of photothermal therapy (PTT) and chemotherapy often induce synergistic effects that markedly exceed the sum of individual treatment alone.⁽³³⁾

The present study is aimed to examine the effect of combined photothermal and nanochemotherapy using gold nanorods (GNR) and nano thymoquinone (NTQ) on chemically-induced OSCC in hamsters. GNRs were used in the present work due to their to convert light into thermal energy, consequently leading to rapid rise of temperature under irradiation with near-infrared (NIR) light⁽³⁴⁾. Thymoquinone (TQ) was used due to its anticancer effect against OSCC⁽³⁵⁾.

In the present study, the prepared polymer PLGA was used as a drug nanocarrier for GNR, NTQ and GNR+NTQ forming a pancake-shaped capsule

with diameter ranges from 115-180 nm. PLGA NPs are widely used as drug delivery system for many therapeutic agents and is favorable for tumor- and/or DNA-targeting⁽³⁶⁾. Folic acid (FA) is a targeting agent as tumor cells over-express their receptors⁽³⁷⁾. In the present study, FA was attached to the PLGA capsule through PEG junction⁽²⁷⁾. This feature seems to work in the current study, where it resulted in significant anti-tumor effect. This conjunction, in the study, depended on Saba et al⁽³⁸⁾ study.

At end of the experiment, animals of DMBA, GNR/NTQ/without laser and NTQ groups showed noticeable decrease in body weight. On the other hand, animals regained weight in GNR/NTQ/laser and GNR/laser groups. It may be due to their therapeutic effect and marked reduction of tumors (size and numbers) in the pouches. Previous studies reported that the DMBA treated-hamsters

had a significant loss of body weight, that might be due to poor food intake, resulting from marked shortening of the painted pouches, as well as tumor overgrowths; so the animals used only the right unpainted pouches for eating^(39,40).

The therapeutic effect of the drugs was assessed by measuring each group's tumor volumes before and after treatments. Significant decrease in tumor volumes, were recorded with the combined therapy (GNR/NTQ) with laser, as well as GNR/laser group. When the tumors were exposed to NIR, the generated heat from the GNRs is transmitted to its surroundings including PLGA shell, NTQ and tumor. Thus, a higher temperature in the PLGA shell could stimulate drug release⁽⁴¹⁾. These results were in line with **Liao et al**,⁽⁴²⁾ who used combined photothermal-nanochemotherapy based on doxorubicin/GNR loaded polymersomes in treatment of C26 cancer cell line. They measured the cytotoxicity of GNRs loaded polymersomes (P/GNRs), doxorubicin co-loaded polymersomes (P/DOX), and GNRs with doxorubicin co-loaded polymersomes (P/GNRs/DOX) with and without NIR laser. Approximately 56 % and 57% of cells were killed by P/DOX and P/GNRs, respectively. After NIR laser irradiation, P/GNRs/ DOX killed 74%. The authors proposed that the greater cytotoxicity of P/GNRs/DOX compared to P/DOX, was primarily a result of enhanced release of DOX upon NIR laser irradiation. GNR/NTQ/no laser and NTQ groups showed significant increase in tumor volumes at the end of the experiment. These results indicated unsatisfactory therapeutic effect of NTQ alone, which may be due to the low dosage given to the animals (only 2 doses). The same with GNR/NTQ/no laser, which attributed to absence of laser irradiation that resulted in no activation of GNRs (required for melting the PLGA capsule)⁽⁴³⁾.

In the present study, histopathological results confirmed cancer regression and tumor volume results. Systemic treatment of the DMBA-painted animals with the combined drug (GNR/NTQ/laser) showed the best therapeutic effect in the form of significant decrease in tumors, with variable degrees of dysplasia. On the other hand, animals treated with GNR/laser showed less improvement in the form of smaller lesions that exhibit carcinoma in situ. GNR/NTQ/no laser and NTQ alone showed the worst results in the form of larger exophytic masses of well to moderate differentiated SCC. These results were in line with other studies^(44,45), in addition to apoptosis and necrosis of cancer cells, hyperthermia also enhances therapeutic efficacy when used with chemotherapy or radiotherapy⁽⁴⁶⁾. Apoptotic cells were identified in H&E sections with GNR/NTQ/laser and GNR/laser groups. Other studies reported the apoptotic and necrotic effect of irradiated GNRs^(47,48), and the apoptotic effect of TQ on malignant cells⁽⁴⁹⁾.

To evaluate the drugs' toxicity, used for treatment, liver and kidney function tests were done. Aspartate aminotransferase (AST) and alanine aminotransferase (ALT) markedly elevated in GNR/NTQ/laser and GNR/laser groups (level of elevation of ALT was less than one fold, and AST was from 2 to 3 folds more than normal). These results suggest that the liver might be affected mildly, due to activated GNRs may have a direct effect on the liver function. Some treatments were found to cause mild elevation in serum AST and ALT levels, due to enzyme induction but not lead to permanent liver damage⁽⁵⁰⁾. Hepatotoxicity causes hepatocellular injury which in turn increases the levels of AST and ALT more than normal (5 to 10 folds)⁽⁵¹⁾. In line with the current results, was **Zhang et al** study⁽⁵²⁾ who recorded an increase in AST and ALT after use of 10 nm and 60 nm of GNPs in rats. Whereas **Saleh et al**⁽⁵³⁾ injected normal hamsters by 18 nm of GNPs

and found no significant elevation in AST and ALT levels. Route of administration, type of laser and the shape of GNPs could affect the results ⁽⁵⁴⁾.

Results of WBCs count significantly increased with GNR/NTQ/laser and GNR/laser groups and highly significantly increased with DMBA, GNR/NTQ without laser, and NTQ groups. The results were in line with **Hassan *et al*** ⁽⁵⁵⁾ and **El Mansy *et al***, ⁽⁴⁰⁾ where the immune-suppressive effect of DMBA could lead to an increase in WBC counts as a defense mechanism. Although GNR/laser group showed clinical and histopathological improvement, it still showed marked elevation of WBC count ⁽⁵⁶⁾. It could be due to their ability to stimulate an inflammatory response ⁽⁵⁷⁾. Of interest, there was a significant improvement of WBCs count with GNR/NTQ/laser group, may be due to the immune-enhancing effect of NTQ ⁴⁰. Platelet count showed no difference between the negative control and GNR/NTQ/laser groups, while increased in DMBA, GNR/laser, GNR/NTQ without laser, and NTQ groups. Platelets have a direct role in cancer ⁽⁵⁸⁾ and the increase in platelet count was directly related to the stage of OSCC. Moreover, it was found that inflammation, infection, iron deficiency anemia and cancer were known to elevate the platelet count ⁽⁵⁹⁾. Decrease in HB and RBCs levels with DMBA, GNR/NTQ without laser, and NTQ groups, while significantly decreased with GNR/NTQ/laser and GNR/laser groups. These results were as **Zhang *et al*** ⁽⁵²⁾ and **Saleh *et al***, ⁽⁵³⁾ who attributed that to the ability of gold nanoparticles to pass through endothelial membrane of the bone marrow, which interfere with the erythropoiesis lead to immature RBCs. **Nithya *et al*** ⁽⁶⁰⁾ reported that restoration of HB contents and RBC count in mice that received TQ after B(a)P-induction, indicated that TQ might protect the tissue from hypoxia and reduced the extent of tumorigenesis.

CONCLUSIONS

The effective ablation of tumor was noticed after i.p injection of two doses of GNR/NTQ/PLGA/FA followed by the irradiation of NIR laser, while NTQ/PLGA/FA or GNR/PLGA/FA/laser alone did not eliminate all tumors. The current findings showed that that combination between photothermal therapy and nonchemotherapy by GNR/NTQ/PLGA/FA was better than either treatment alone.

ACKNOWLEDGMENT

We are grateful to Dr Wael Darwish in national research Centre for preparation and characterization of drug formulations and laser setting utilized in this work

REFERENCES

1. Siegel RL, Miller KD, Jemal A. Cancer statistics, 2019. *CA Cancer J Clin.* 2019; 69 :7-34.
2. Warnakulasuriya S. Global epidemiology of oral and oropharyngeal cancer. *Oral Oncol.* 2009; 45: 309-316.
3. Tanaka T, Ishigamori R. Understanding carcinogenesis for fighting oral cancer. *J Oncol.* 2011; 2011: 603740.
4. Marsh D, Suchak K, Moutasim KA, Vallath S, Hopper C, Jerjes W, Upile T, Kalavrezos N, Violette SM, Weinreb PH, Chester KA, Chana JS, Marshall JF, Hart IR, Hackshaw AK, Piper K, Thomas GJ. Stromal features are predictive of disease mortality in oral cancer patients. *J Pathol.* 2011; 223:470-481.
5. Liao YT, Liu HC, Chin,Y, Chen YS, Liu HS, Hsu CY. Biocompatible and multifunctional gold nanorods for effective photothermal therapy of oral squamous cell carcinoma. *J Mater Chem B.* 2019; 7:4451-4460.
6. Wu T, Zhou S. Nanoparticle-based targeted therapeutics in head-and-neck cancer. *Int J Med Sci* 2015; 12:187-200.
7. Gimenez-Conti IB, Slaga TJ. The hamster cheek pouch carcinogenesis model. *J Cell Biochem (Suppl.)*.1993; 17: 83-90.

8. Nagini S, Letchoumy P, Thangavelu A, Ramachandran CR. Of humans and hamsters: The hamster buccal pouch carcinogenesis model as a paradigm for oral oncogenesis and chemoprevention. *Anticancer Agents Med Chem.* 2009; 9: 843-852.
9. Goyal SN, Prajapati CP, Gore PR, Patil CR, Mahajan UB, Sharma C, Talla SP, Ojha SK. Potential, and pharmaceutical development of thymoquinone: a multitargeted molecule of natural origin. *Front Pharmacol.* 2017; 8:656- 875.
10. Mostofa AGM, Hossain K, Basak D, Bin Sayeed M. Thymoquinone as a potential adjuvant therapy for cancer treatment: evidence from preclinical studies. *Front Pharmacol.* 2017; 8:295-307.
11. Alkharfy KM, Ahmad A, Khan RM, Al-Shagha WM. Pharmacokinetic plasma behaviors of intravenous and oral bioavailability of thymoquinone in a rabbit model. *Eur J Drug Metab Pharmacokinet.* 2015; 40:319-323.
12. Nair HB, Sung B, Yadav VR, Kannappan R, Chaturvedi MM, Aggarwal BB. Delivery of anti-inflammatory nutraceuticals by nanoparticles for the prevention and treatment of cancer. *Biochem Pharmacol.* 2010; 80:1833-1843.
13. Schneider-Stock R, Fakhoury IH, Zaki AM, El-Baba CO, Gali-Muhtasib HU. Thymoquinone: Fifty years of success in the battle against cancer models. *Drug Discov Today.* 2014; 19: 18-30.
14. Huang X, Jain PK, El-Sayed IH, El-Sayed MA. Plasmonic photothermal therapy (PPTT) using gold nanoparticles. *Lasers Med Sci.* 2008; 23:217-228.
15. Zhang H, Salo D, Kim DM, Komarov S, Tai Y, Berezin MY. Penetration depth of photons in biological tissues from hyperspectral imaging in shortwave infrared in transmission and reflection geometries. *J Biomed Opt.* 2016; 21: 126006-126016.
16. Tchounwou C, Sinha SS, Viraka Nellore BP, Pramanik A, Kanchanapally R, Jones S, Chavva SR, Ray PC. Hybrid theranostic platform for second near-IR window light triggered selective two-photon imaging and photothermal killing of targeted melanoma cells. *ACS Appl Mater Interfaces.* 2015; 7:20649-20656.
17. Tong L, Zhao Y, Huff TB, Hansen MN, Wei A, Cheng JX. Gold nanorods mediate tumor cell death by compromising membrane integrity. *Adv Mater.* 2007; 19: 3136-3141.
18. Weissleder R. A clearer vision for in vivo imaging. *Nat Biotechnol.* 2001; 19:316-317.
19. Lee SM, Kim HJ, Kim SY. Drug-loaded gold plasmonic nanoparticles for treatment of multidrug resistance in cancer. *Biomater.* 2014; 35:2272-2282.
20. Liopo AV, Conjusteau A, Chumakova OV, Ermilov SA, Su R, Oraevsky AA. Highly purified biocompatible gold nanorods for contrasted optoacoustic imaging of small animal models. *Nanosci Nanotechnol Lett.* 2012; 4:681-686.
21. Riley R, Day E. Gold nanoparticle-mediated photothermal therapy: applications and opportunities for multimodal cancer treatment. *Nanomed Nanobiotechnol.* 2017; 9: e1449.
22. Raeesi V, Chan WCW. Improving nanoparticle diffusion through tumor collagen matrix by photo-thermal gold nanorods. *Nanoscale.* 2016; 8:12524-12530.
23. Fay BL, Melamed JR, Day ES. Nanoshell-mediated photothermal therapy can enhance chemotherapy in inflammatory breast cancer cells. *Int J Nanomed.* 2015; 10:6931-6941..
24. Nayak S, Lee H, Chmielewski J, Lyon LA. Folate mediated cell targeting and cytotoxicity using thermo responsive microgels. *J Am Chem Soc.* 2004; 126:10258-10259.
25. Yoo H, Park T. Folate-receptor-targeted delivery of doxorubicin nano-aggregates stabilized by doxorubicin-peg-folate conjugate. *J Control Release.* 2004; 100:247-256.
26. Parker N, Turk MJ, Westrick E, Lewis JD, Low PS, Leamon CP. Folate receptor expression in carcinomas and normal tissues determined by a quantitative radioligand binding assay. *Anal Biochem.* 2005; 338: 284-293.
27. Muller C, Schibli R. Folic acid conjugates for nuclear imaging of folate receptor-positive cancer. *J Nucl Med.* 2011; 52:1-4.
28. Silva A, Cardoso B, Silva M, Freitas R, Sousa R. Synthesis, characterization, and study of PLGA copolymer in vitro degradation. *J Biomater Nanobiotechnol.* 2015; 6 :8-19.
29. Liu H, Zhao M, Wang, J, Pang M, Wu Z, Zhao L, Yin Z, Hong Z. Photodynamic therapy of tumors with pyropheophorbide-a-loaded polyethylene glycol-poly(lactico-glycolic acid) nanoparticles. *Int J Nanomed.* 2016; 11: 4905-4918.

30. Sau TK, Murphy CJ. Seeded high yield synthesis of short Au nanorods in aqueous solution. *Langmuir*. 2004; 20: 6414-6420.
31. Shklar G. The effect of manipulation and incision on experimental carcinoma of hamster buccal pouch. *Cancer Res*. 1968; 28:2180-2182.
32. Faustino-Rocha A, Oliveira PA, Teixeira-Guedes C, Soares-Maia R, Pires MJ, Ferreira R and Ginja M. Estimation of rat mammary tumor volume using caliper and ultrasonography measurements. *Lab Anim* 2013; 42:217-224.
33. Khafaji M, Zamani M, Golizadeh M, Bavi O. Inorganic nanomaterials for chemo/photothermal therapy: a promising horizon on effective cancer treatment. *Biophys Rev* 2019; 11: 335-352.
34. Dickerson EB, Dreaden EC, Huang X, El-Sayed IH, Chu H, Pushpanketh S, McDonald JF, El-Sayed MA. Gold nanorod assisted near-infrared plasmonic photothermal therapy (PPTT) of squamous cell carcinoma in mice. *Cancer Lett*. 2008; 269:57-66.
35. Chu SH, Hsieh YH, Yu CC, Lai YY, Chen PN. Thymoquinone induces cell death in human squamous carcinoma cells via caspase activation-dependent apoptosis and LC3-II activation-dependent autophagy. *PLoS One*. 2014; 9: 101579-101589.
36. Berthet M, Gauthier Y, Lacroix C, Verrier B, Monge C. Nanoparticle-based dressing: the future of wound treatment? *Trends. Biotechnol*. 2017; 35:770-784.
37. Fernández M, Javaid F, Chudasama V. Advances in targeting the folate receptor in the treatment/imaging of cancers. *Chem Sci*. 2018; 9:790-810.
38. Saba NF, Wang X, Müller S, Tighiouart M, Cho K, Nie S, Chen Z, Shin DM. Examining expression of folate receptor in squamous cell carcinoma of the head and neck as a target for a novel nanotherapeutic drug. *Head Neck*. 2009; 31(4):475-481.
39. El-Sherbiny R, Hassan MA, Korraa A. Effect of different nanothymoquinone concentrations on the chemically-induced epithelial dysplasia in the hamster buccal pouch. *SCU Med J*. 2017; 20: 75-89.
40. *El-Mansy M, Hassan M, Abou Elnour K*. Treatment of oral squamous cell carcinoma using thymoquinone loaded on gold nanoparticles. *SCU Med J*. 2017; 20 :119-1.
41. Chuang CC, Cheng CC, Chen PY, Lo C, Chen YN, Shih MH, Chang CW. nanorod-encapsulated biodegradable polymeric matrix for combined photothermal and cancer therapy. *Int J Nanomed*. 2019; 14:181-193.
42. Liao J, Li W, Peng J, Yang Q, Li H, Wei Y, Zhang X, Qian Z. Combined cancer photothermal-chemotherapy based on doxorubicin/gold nanorod-loaded polymersomes. *Theranostics*. 2015; 5:345-356.
43. Sheng G, Chen Y, Han L, Huang Y, Liu X, Li L, Mao Z. Encapsulation of indocyanine green into cell membrane capsules for photothermal cancer therapy. *Acta Biomater*. 2016; 43:251-261.
44. Chen J, Li X, Zhao X, Wu Q, Zhu H, Mao Z, Gao C. Doxorubicin-conjugated pH-responsive gold nanorods for combined photothermal therapy and chemotherapy of cancer. *Bioact Mater*. 2018; 3:347-354.
45. Wang B, Wang JH, Liu Q, Huang H, Chen M, Li K, Li C, Yu XF, Chu PK. Rose-bengal-conjugated gold nanorods for in vivo photodynamic and photothermal oral cancer therapies. *Biomaterials*. 2014;35:1954-1966.
46. Kampinga H. Cell biological effects of hyperthermia alone or combined with radiation or drugs: a short introduction to newcomers in the field. *Int J Hyperthermia* 2006; 22:191196.
47. Kim M, Kim G, Kim D, Yoo J, Kim DK, Kim H. Numerical study on effective conditions for the induction of apoptotic temperatures for various tumor aspect ratios using a single continuous-wave laser in photothermal therapy using gold nanorods. *Cancers (Basel)*. 2019;11:pii: E764.
48. Pattani V, Shah J, Atalis A, Sharma A, Tunnell J. Role of apoptosis and necrosis in cell death induced by nanoparticle-mediated photothermal therapy. *J Nanopart Res* 2015: 17:20:1-11.
49. Abdelfadil E, Cheng YH, Bau DT, Ting WJ, Chen LM, Hsu HH, Lin YM, Chen RJ, Tsai FJ, Tsai CH, Huang CY. Thymoquinone induces apoptosis in oral cancer cells through p38 β inhibition. *Am J Chin Med* 2013; 41: 683-696.
50. Malakouti M, Kataria A, Ali S, Schenker S. Elevated liver enzymes in asymptomatic patients—what should I do? *J Clin Transl Hepatol* 2017; 5: 394–403.

51. Dufour D, Lott J, Nolte F, Gretch D, Koff R, Seeff L. Diagnosis and monitoring of hepatic injury. II. Recommendations for use of laboratory tests in screening, diagnosis, and monitoring. *Clin Chem* 2000; 46: 2050-2068.
52. Zhang XD, Wu HY, Wu D, Wang YY, Chang JH, Zhai ZB. Toxicologic effects of gold nanoparticles in vivo by different administration routes. *Int J Nanomed* 2010; 5: 771-781.
53. Saleh H, Soliman O, Elshazly M, Raafat A, Gohar A, Salaheldin T. Acute hematologic, hepatologic, and nephrologic changes after intraperitoneal injections of 18 nm gold nanoparticles in hamsters. *Int J Nanomed* 2016; 11: 2505-2513.
54. Abdoon A, Al-Ashkar E, Kandil O, Shaban A, Khaled H, El Sayed M, El Shaer M, Shaalan A, Eisa W, GamalEldin A, Hussein H, El Ashkar M, Ali M, Shabaka A. Efficacy and toxicity of plasmonic photothermal therapy (PPTT) using gold nanorods (GNRs) against mammary tumors in dogs and cats. *Nanomed Nanotechnol Biol Med* 2016; 12: 2291-2297.
55. Hassan MA, Abou El-Nour KM, El-Azab MF, Shata MS. Nano-chemoprevention of oral squamous cell carcinoma using thymoquinone loaded on gold nanoparticles. *Proc. ICNA. Feb. 22nd-25th, Hurghada, Egypt. 2016.*
56. Das S, Debnath N, Mitra S, Datta A, Goswami A. Comparative analysis of stability and toxicity profile of three differently capped gold nanoparticles for biomedical usage. *Biometals* 2012; 25:1009-1022.
57. Dwivedi PD, Tripathi A, Ansari KM, Shanker R, Das M. Impact of nanoparticles on the immune system. *J Biomed Nanotechnol* 2011; 7:193-194.
58. Ho-Tin-Noé B, Demers M, Wagner DD. How platelets safeguard vascular integrity. *J Thromb Haemost* 2011; 9:56-65.
59. Buergy D, Wenz F, Groden C, Brockmann MA. Tumor-platelet interaction in solid tumors. *Int J Ca* 2012; 130: 2747-2760.
60. Nithya G, Mani R, Sakthisekaran D. Oral administration of thymoquinone attenuates benzo (a) pyrene-induced lung carcinogenesis in male Swiss albino mice. *Int J Pharm Pharm Sci* 2014; 6: 260-263.